Full Paper

Israel Journal of Chemistry

DOI: 10.1002/ijch.201300106

Stereoselective Diels–Alder Reactions Promoted under Continuous-Flow Conditions by Silica-Supported Chiral Organocatalysts

Riccardo Porta, Maurizio Benaglia,* Valerio Chiroli, Francesca Coccia, and Alessandra Puglisi[a]

Abstract: Silica nanoparticles of different morphological properties were functionalized with enantiomerically pure imidazolidinones, through different immobilization techniques; stainless-steel columns were then loaded with silica bearing chiral organocatalysts to realize chiral "homemade" reactors. The influence of the material properties and immobilization procedures on the chemical and stereochemical activities of the chiral HPLC columns was studied by performing organocatalyzed Diels–Alder reactions between cyclopentadiene and α,β-unsaturated aldehydes under continuous-flow conditions. In some cases, excellent enantioselectivities were obtained, thus showing that a catalytic reactor may work efficiently to continuously produce enantiomerically enriched cycloadducts for more than 200 h. Regeneration of the organocatalytic column was also partially accomplished, although associated with a slightly lower enantioselectivity, thus prolonging the "life" of the reactor to more than 300 h.

Keywords: Chirality · Cycloaddition · Flow chemistry · Organocatalysis · Supported catalysts

1 Introduction

In the last twenty years, organic synthesis has somehow been revolutionized by the advent of automation and new advanced technologies able to facilitate the process of preparation and isolation of a product.[1] For example, solid-phase-assisted synthesis,[2] largely employed in the pharmaceutical and medicinal chemistry, is only one of the so-called enabling technologies developed with the aim of speeding up the synthetic transformation and purification of the final product.[3]

In this context, it must be seen the extraordinary opportunity offered by the development and the design of new reactors, such as continuous-flow and micro reactors.[4] Microreactor technology offers advantages to classical approaches by allowing miniaturization of structural features up to the micrometer regime. In recent years, chemists have recognized this as a very powerful tool and many reactions have been performed in such devices. These reactions benefit from the physical properties of microreactors, such as enhanced mass and heat transfer due to a very large surface to volume ratio, as well as regular flow profiles, leading to improved yields with increased selectivities.[5] Also, the recent developments and excellent results obtained in the synthesis of fine chemicals and complex molecules in flow[6] represent a clear demonstration of the exciting possibilities given from the new technological platforms for both homo- and heterogeneous transformations.[7]

In this regard, the use of immobilized chiral catalysts[8] under flow conditions is extremely attractive, since it presents several advantages over traditional batch process, such as easy product purification procedures, improved catalyst stability, and the possibility of designing automated processes.[9] Chiral organic catalysts have an additional positive feature: the metal-free nature of these compounds avoids, from the outset, the problem of metal leaching, which often negatively affects and practically prevents the efficient recycling of a supported organometallic catalyst and may lead to product contamination by the metal.

However, surprisingly, although in the last decade incredibly intense activity focused on the use of different chiral organometallic catalysts under flow conditions, only a few examples of chiral organocatalysts were investigated.[10] After the pioneering work by Lectka et al. with polystyrene-immobilized cinchona alkaloid derivatives,[11] very recently the groups of Pericàs and Massi have studied the use of polymer-supported proline[12] and prolinol[13] derivatives in mini flow reactors. Lately, the groups of Fulop[14] and Wennemers[15] have reported stereoselective Michael additions promoted in continuo by polymer-supported tripeptides. It should be noted that all

[a] R. Porta, M. Benaglia, V. Chiroli, F. Coccia, A. Puglisi
Dipartimento di Chimica, Università degli Studi di Milano, Via Golgi 19, 20133, Milan (Italy)
e-mail: maurizio.benaglia@unimi.it

Supporting information for this article is available on the WWW under http://dx.doi.org/10.1002/ijch.201300106.

of these works were almost exclusively limited to the use of packed-bed reactors filled with catalyst supported on inorganic or gel-type organic materials, with substrate activation via enamine intermediates.

We recently reported on the preparation of a "home-made" silica-based HPLC column,[16] functionalized with a supported enantiomerically pure organic catalyst, that promoted stereoselective reactions via an iminium intermediate. The silica-supported MacMillan catalyst was employed for the first time to perform stereoselective cycloaddition under continuous-flow conditions, in high yields and enantioselectivities. The so-called MacMillan catalysts are chiral imidazolidinones, which are one of the most popular and versatile classes of chiral metal-free catalysts.[17] These compounds have been covalently immobilized both on soluble[18] and insoluble supports.[19] Lately, properly modified enantiopure imidazolidinones were anchored to novel siliceous mesocellular foams,[20] and to silica gel with the aid of an ionic liquid,[21] while in another work hollow periodic mesoporous organosilica spheres were exploited.[22] Recently, Pericàs and co-workers reported the anchoring of first-generation MacMillan imidazolidinone onto polystyrene resins and magnetic nanoparticles[23a] and our group also reported the use of magnetic nanoparticles conjugated to chiral imidazolidinone as a recoverable catalyst.[23b] Despite this variety of proposed solutions, however, the development of an easily available, inexpensive, truly efficient, recoverable MacMillan catalyst has still to be realized. Lower enantioselectivities with respect to those of the nonsupported system and recyclability are issues that are still waiting for a satisfying solution: the use of MacMillan catalysts in reactors under continuous-flow conditions might open up interesting perspectives and new solutions to these issues.

Based on our previous experience,[24] and taking the good preliminary results obtained by using commercial silica-supported catalysts under continuous-flow conditions into consideration,[16] we decided to further investigate the use of these materials in stereoselective cycloadditions performed in flow. Herein, we report the preparation of silica-supported MacMillan catalysts through different immobilization strategies, the characterization of the functionalized materials, and the study of their catalytic behavior in a stereoselective Diels–Alder reaction under continuous-flow conditions.

2 Results and Discussion

2.1 Synthesis of Silica-Supported Catalysts

The use of (*S*)-tyrosine instead of (*S*)-phenylalanine to generate an imidazolidinone offers the possibility to synthesize the desired chiral catalyst, which is already equipped with a properly located and chemically suitable handle for the heterogenization process (Figure 1).[18]

Thus, starting from (*S*)-tyrosine methyl ester hydrochloride, imidazolidinone **1** was easily obtained in 77 % yield by *N*-butyl amide formation and treatment with acetone (Scheme 1). Reaction with allyl bromide in acetonitrile in the presence of Cs_2CO_3 allowed the introduction of the carbon–carbon double bond, which was further functionalized by platinum-catalyzed hydrosilylation, leading to compound **2**, featuring the key structural element to realize catalyst immobilization. Grafting of functionalized

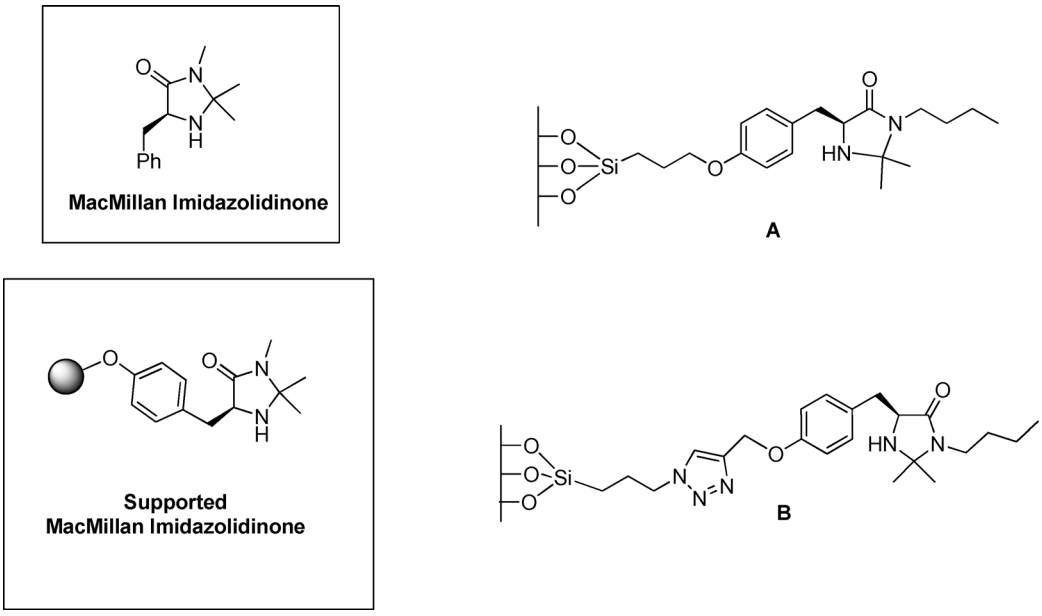

Figure 1. MacMillan catalyst and silica-supported imidazolidinones.

Israel Journal of Chemistry

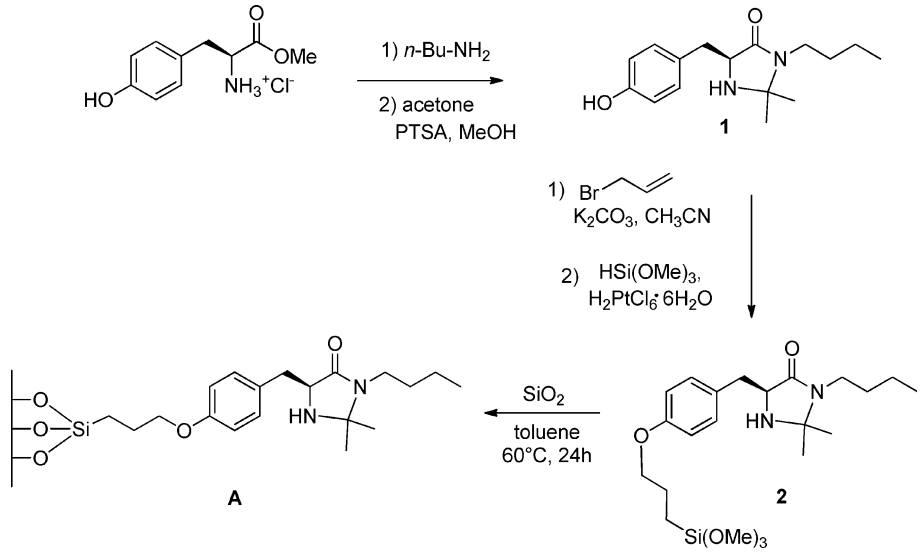

Scheme 1. Synthesis of supported imidazolidinone type **A**. PTSA = *p*-toluenesulfonic acid.

imidazolidinone **2** onto silica nanoparticles in toluene at 60 °C for 24 h afforded supported catalyst type **A**.

With regard to catalyst type **A**, three types of commercially available silica were used as supports (particle sizes of 8, 10, and 25 μm) to study the influence of the morphological properties on the catalytic behavior. However, preliminary studies convinced us to focus our attention on the first two silica types only (particle size of 8 and 10 μm). Materials of different morphological properties were purchased from different companies: catalyst **A8-1** was prepared by grafting imidazolidinone **2** onto Apex Prepsil Silica Media 8 μm (Grace Davison – Discovery Sciences, asymmetry 0.9, pore diameter 120 Å, mean particle size 8.4 μm, and surface area 162 m^2/g), obtaining a loading of 0.39 mmol/g (determined by weight difference of the materials before and after grafting; see below for further characterization details). To study the influence of the catalyst loading on the catalyst performances, two other functionalized materials were prepared using 8 μm silica, namely, material **A8-2** (loading of 0.33 mmol/g) and catalyst **A8-3** (loading of 0.1 mmol/g). Catalyst **A10-1** was prepared by grafting imidazolidinone **2** onto Luna Silica 10 μm (pore diameter 101 Å, mean particle size 8.57 μm, and surface area 380 m^2/g); the loading was found to be 0.53 mmol/g (see below for further details).

Following the same strategy, catalyst type **B** was also easily prepared by reacting the same intermediate **1** with propargyl bromide and imidazolidinone **3**, bearing a carbon–carbon triple bond, was obtained after a single chromatographic purification step (Scheme 2).

The modified MacMillan catalyst was then reacted with the properly derivatized siliceous material; siloxane **4** was readily prepared from commercially available 3-chloropropyl triethoxysilane and sodium azide in CH_3CN, and grafted to the commercially available 8 μm silica nanoparticles to afford silica-supported azide **5**, which was subjected to copper-catalyzed cycloaddition with derivative **3** to give catalyst **B1**. The same intermediate **4** was also employed to prepare a mesoporous azide-functionalized silica (**5-MSN**) through a co-condensation method. Starting from the modified MacMillan catalyst **3**, a click chemistry strategy allowed the preparation of a chiral organocatalyst anchored to a mesoporous silica material, **B2**. After the copper(I)-catalyzed click reaction, the materials were washed with ammonia solution and analyzed by energy-dispersive X-ray spectroscopy (EDX), which showed no traces of residual copper.[25]

2.2 Characterization of Supported Catalysts

The supported catalysts were characterized by performing cross-polarization (CP) and direct-polarization (DP) magic-angle spinning (MAS) ^{13}C and ^{29}Si NMR spectroscopy experiments to obtain evidence for the presence of the organic moieties in the siliceous materials and confirm their chemical structure.

2.2.1 ^{13}C CPMAS NMR Spectroscopy

The ^{13}C spectra of the prepared catalysts demonstrated that the materials were indeed functionalized as expected and the organic residues were stably bound to the inorganic material (see the chemical shifts of carbon atoms C-1 and C-3). For comparison, we report the ^{13}C resonances of catalyst **A10-1**, in which the imidazolidinone moiety is directly linked to the silica surface, and catalyst **B2**, bearing a triazole spacer between the imidazolidinone and the silica surface. The ^{13}C resonances reported in Table 1 are assigned based on the chemical shifts found in the solution spectra of organic precursors (see the Experimental Section and the Supporting Information).

Israel Journal of Chemistry

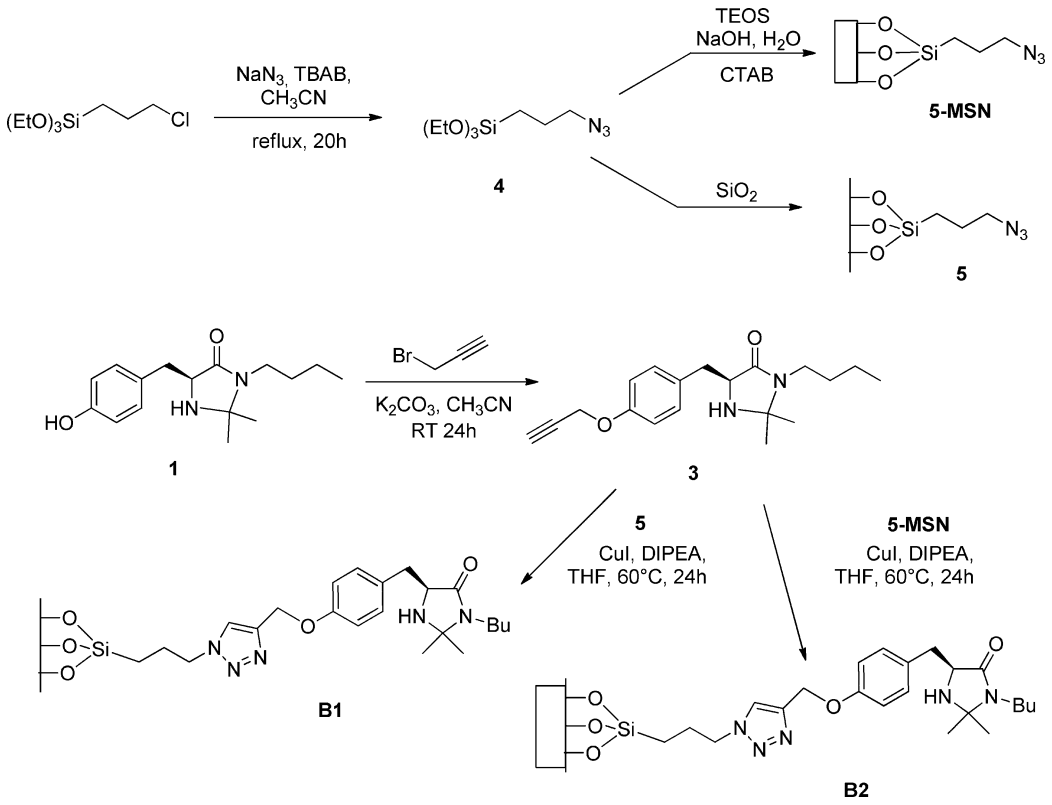

Scheme 2. Synthesis of supported azide **5** and supported catalyst type **B**. TBAB = tetra-*n*-butylammonium bromide, TEOS = tetraethoxysilane, CTAB = cetyltrimethylammonium bromide, DIPEA = *N*,*N*-diisopropylethylamine.

Table 1. ^{13}C NMR resonances [ppm] in the solid-state spectra of catalysts **A10-1** and **B2**.

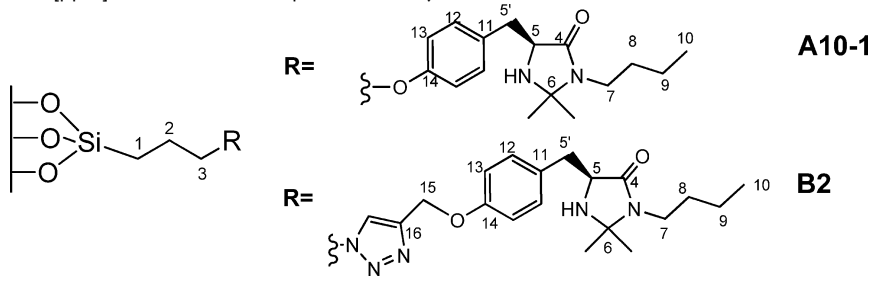

	C1	C2	C3	C4	C5	C5′	C6	C7	C8	C9	C10	C11	C12	C13	C14	C15	C16
A10-1	7.60	22.1	68.8	175.2	58.5	39.3	76.2	50.7	31.4	19.7	11.5	130.2	130.2	114.7	158.4		
B2	9.0	23.0	51.8	174.0	58.0	40.0	76.0	50.0	28.0	19.7	13.0	129.0	129.0	114.0	157.4	62.0	143.3

As expected, based on previous experiments, the ^{13}C spectrum of catalyst **B2**, synthesized by cycloaddition of imidazolidinone **3** with the supported azide **5-MSN**, revealed about 25% of unreacted azide starting material. The ratio between the two organic moieties (the azide and the imidazolidinone) can be calculated by integrating the signal of carbon atoms C-1 (9.0 ppm) and C-10 (13.0 ppm). (The data should be considered within the limit of the analytical technique.)

2.2.2 ^{29}Si DP and CPMAS NMR Spectroscopy

The ^{29}Si NMR spectra of siliceous materials are extensively used to determine the degree of functionalization of the materials, as well as to give insights into the substitution of the surface silicon atoms. It is well recognized that a given surface silicon atom bearing a functional group can have a variable number, *n*, of Si-O-Si bonds, leading to so-called T_1, T_2, and T_3 substructures. The bonding schemes for these hybrid materials containing organic functionalities lead to very different geometries on the

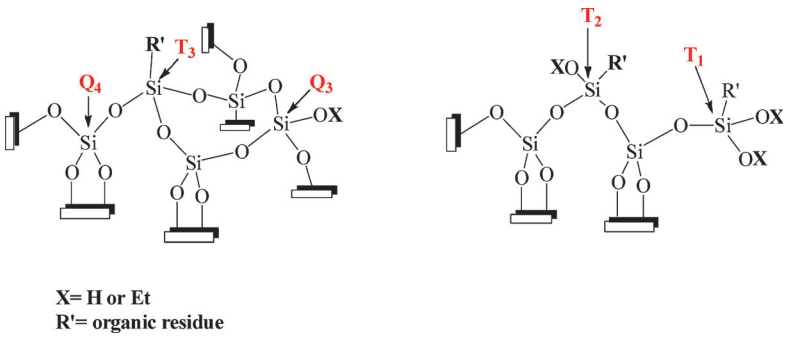

Figure 2. Possible Si substitution on the silica surface.

surface, as illustrated in Figure 2. The ^{29}Si spectra also gives information about the bulk surface species Q_4 ($(SiO)_4$ Si) and proton-rich Q_n sites: Q_3 ($(SiO)_3$ SiOH), Q_2 ($(SiO)_2$ Si$(OH)_2$), and Q_1 ((SiO) Si$(OH)_3$; Figure 2). Knowledge of the surface incorporation patterns and the conformations of functional groups for such materials is an essential step toward developing efficient functional substrates.

^{29}Si DP/MAS experiments, carried out according to previously described methods,[26] were performed in this study for the prepared catalysts. As expected, the ^{29}Si solid-state spectra are dominated by resonance lines at −113, −103 and −96 ppm, representing silicon sites Q_4, Q_3, and Q_2 , respectively. On the other hand, different patterns were found in the spectra of the catalysts with regard to the functionalized T_n species, in which the silicon atoms were directly bound to at least one organic moiety.

The presence of signals assigned to T_3, T_2, and T_1 confirmed that the organic groups were indeed covalently bound to the surface. Quantitative measurements of T_n and Q_n silicon groups could be properly achieved by ^{29}Si DP/MAS experiments, as reported previously,[24,26] to determine the relative concentrations of T_n and Q_n, surface coverage, and molar concentrations of the organic moieties. For comparison, in Table 2 we report the data of catalyst **A10-1**, in which the imidazolidinone moiety is directly linked to the silica surface, and catalyst **B2**, bearing a triazole spacer between the imidazolidinone and the silica surface.

Notably, catalyst **B2** has a larger surface coverage, estimated as SC=$(T_1+T_2+T_3)/(Q_2+Q_3+T_1+T_2+T_3)$, due the structure of the siliceous material, in which the organic moiety can cover the interior wall of the mesopores. Catalyst **A10-1**, derived from grafting of a trialkoxysilane to a commercially available silica, presents smaller T_2 and T_3 values, leading to a smaller SC. In the case of **A10-1**, the calculated loading (MC) is in good agreement with that obtained by weight difference of a silica sample before and after functionalization (0.67 vs. 0.53 mmol/g); the MC of **B2**, on the other hand, is overestimated (0.95 vs. 0.40 mmol/g). Even if in the quantification of organic residues on silica matrix some discrepancies among different analytical techniques arise, MAS-NMR spectroscopy remains a powerful method for the characterization of functionalized siliceous materials, since it can be used not only to study different surface incorporation patterns, but also to determine the ratio between two different organic residues.

2.2.3 Morphological Properties

The morphological examination of the sample particles was performed by collecting images of the surfaces by SEM analysis. The images of the surfaces of all of the inorganic–organic hybrid materials compared with those of bare silica showed a variety of particle shapes and sizes densely agglomerated.

Figure 3 presents the SEM image of catalyst **B1**: the micrograph clearly shows some aggregation of the material; this particle aggregation can explain the experimental observation that, after prolonged fluxing of the column (six volumes of column), no reagents or products, pre-

Table 2. ^{29}Si DP/MAS NMR chemical shifts, relative concentrations of T_n and Q_n silicon groups (in %), surface coverage (SC, in %), and molar concentrations of organic moieties (MC, in mmol/g) of catalysts **A10-1** and **B2**.

Catalyst	T_1 % −54 ppm	T_2 % −60 ppm	T_3 % −68 ppm	Q_2 % −96 ppm	Q_3 % −103 ppm	Q_4 % −113 ppm	SC [%]	MC [mmol/g]
A10-1	–	2.5	2.8	0	22.5	72.2	19.1	0.67
B2	–	4.1	13.0	4.4	30.5	48.0	33.0	1.43[a]

[a] Overall (catalyst + azide).

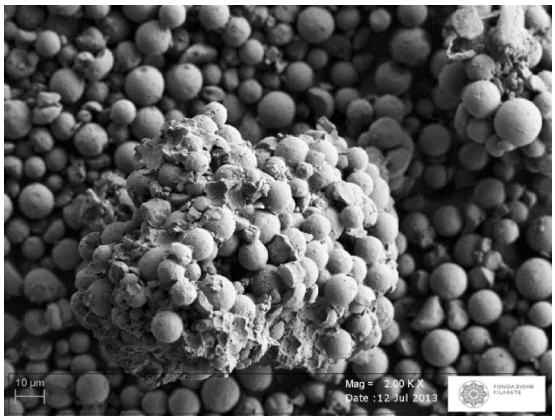

Figure 3. SEM image of a sample of catalyst **B1**.

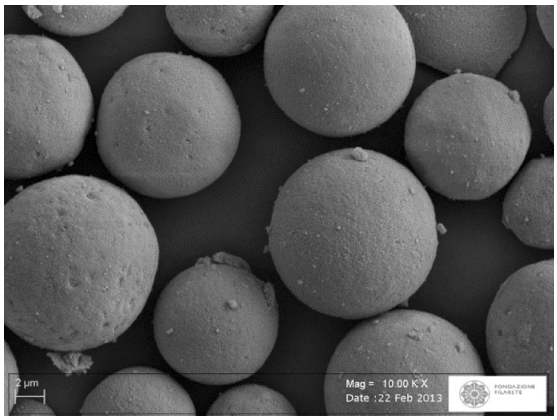

Figure 5. SEM image of a sample of catalyst **A8-1**.

sumably retained inside the reactor, were detected at the exit (see below for catalytic experiments).

Figure 4 shows the micrographs of catalyst **B2** at two different magnifications: as expected,[24] rod-shaped particles of different lengths and diameters (ca. 0.4 µm in length and 500 nm in diameter), with a curved hexagonal-shaped tubular morphology, completely cover irregular polyhedral-shaped grains associated with the silica morphology.

A SEM image of catalyst **A8-1** (Figure 5) shows a regular distribution of particle sizes and confirms that no mechanical degradation occurs after functionalization of the siliceous material.

2.3 Catalytic Behavior of the Immobilized Catalysts

The behavior of silica-anchored imidazolidinones type **A** and **B** was first investigated by running a model reaction in batch; Diels–Alder cycloaddition between cinnamic aldehyde (1 equiv) and cyclopentadiene (5 equiv) in CH_3CN/H_2O as a solvent system using 30 mol% of the supported catalyst was performed for 40 h at 25 °C in the presence of different acid additives. A few selected results are summarized in Table 3.

Since MacMillan catalyst requires an acidic additive, among different possibilities, we focused on the use of tetrafluoroboric (HBF_4) and trifluoroacetic acid (TFA). In explorative studies it was noted that pre-forming the catalyst led to a marked decrease of both yield and stereoselection; therefore, in situ addition of the acid to the reaction mixture was preferred.

Catalyst **A8-1** afforded the cycloadducts in 75% yield with 75% *ee* for the *endo* isomer and 76% *ee* for the *exo* isomer, in the presence of tetrafluoroboric acid as an additive; comparable yields and slightly better enantioselectivities were observed with trifluoroacetic acid.[27] It should be mentioned that the *endo*/*exo* ratio remained almost unvaried in all catalytic reactions and was comparable to the ratio obtained by the original MacMillan imidazolidinone.[28] Very similar results were obtained with the catalyst anchored to 10 µm silica nanoparticles, **A10-1** (Table 3, entries 3 and 4 versus entries 1 and 2). When recycling of the supported imidazolidinones was studied,

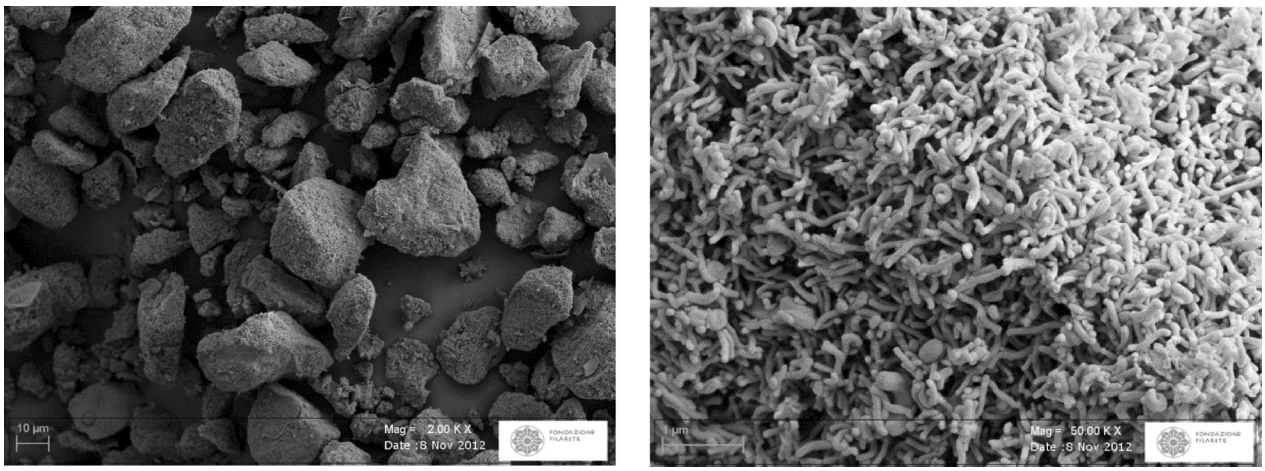

Figure 4. SEM images of a sample of catalyst **B2** magnified at 2000× (left) and 50000× (right).

Table 3. Diels–Alder reactions promoted by catalysts type **A** and **B** in batch.

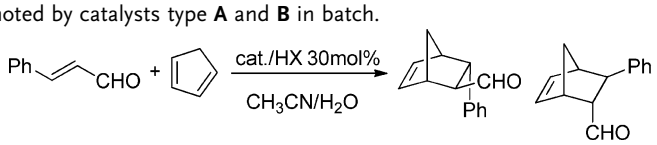

Entry	Catalyst	HX	Yield [%][a]	*endo*/*exo*[b]	*ee* [%] (*endo*,*exo*)[c]
1	**A8-1**	HBF_4	75	53 : 47	75, 76
2	**A8-1**	TFA	69	51 : 49	80, 82
3	**A10-1**	HBF_4	78	52 : 48	78, 77
4	**A10-1**	TFA	66	53 : 47	83, 86
5[d]	**A10-1**	HBF_4	15	55 : 45	n.d.
6[d]	**A10-1**	TFA	12	56 : 44	n.d.
7	**B2**	HBF_4	75	54 : 46	91, 89
8	**B2**	TFA	52	55 : 45	87, 97
9[e]	**B2**	HBF_4	91	55 : 45	93, 91

[a] Reaction conditions: 48 h, 25 °C, isolated yield after chromatographic purification. [b] Evaluated by ^{1}H NMR spectroscopy on the crude reaction mixture. [c] Evaluated by HPLC on a chiral stationary phase after reduction to the corresponding alcohol. [d] Recovered supported catalyst was employed. [e] A second portion of cyclopentadiene was added after the first 24 h.

disappointingly an evident decrease in the chemical yield was detected, which was a clear indication of rapid catalyst deactivation after only 48 h.

MacMillan catalyst immobilized through click chemistry on silica showed similar chemical activity, but promoted the cycloaddition with higher enantioselectivities, comparable to those obtained with the non-supported organocatalysts.[28]

Then the same materials were employed to promote stereoselective Diels–Alder under continuous-flow conditions. A standard HPLC column (0.4 cm i.d. × 12.5 cm, 1.6 mL total volume) was filled with functionalized silica nanoparticles. Tetrafluoroborate salt of catalyst **A8-1** was first studied (Table 4).

A conditioning time was necessary to reach a steady-state regime of high chemical and stereochemical activities; probably an effective exchange between the solid-supported catalyst and the liquid phase containing the reactants must be realized before the column may work efficiently. As also demonstrated by the reaction under batch conditions, after 24 h only 50 % yield was observed, and longer reaction times were necessary to reach higher yields. However, after the first 22 h, the column produced for the next 8 h the product with constant yield, although with low enantioselectivity; lowering the flow rate allowed the stereoselectivity of the process to be improved, without loss in chemical yield. Indeed, after the first 30 h, the reactor produced the cycloadducts with yields constantly higher than 91 % and enantioselectivities typically

Table 4. Diels–Alder reaction promoted by catalyst type **A8-1** under continuous-flow conditions.

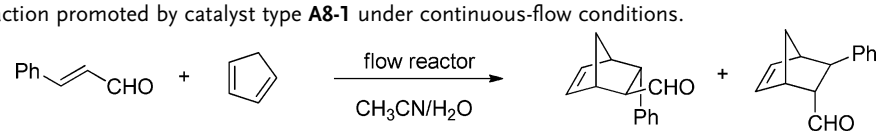

Entry	*t* [h]	Flow rate [µL/min]	Residence time [h]	HX	Yield [%][a]	*endo*/*exo*[b]	*ee* [%] (*endo*,*exo*)[c]
1	10–22	2.5	10	HBF_4	45	46:54	38, 58
2	22–26	2.5	10	HBF_4	86	47:53	47, 60
3	26–30	2.5	10	HBF_4	88	47:53	49, 63
4	30–50	1.5	16.5	HBF_4	91	47:53	71, 73
5	50–96	1.5	16.5	HBF_4	92	42:58	85, 81
6	96–150	1	25	HBF_4	95	44:56	83, 80
7	10–20	2.5	10	TFA	94	48:52	85, 85
8	20–96	2.5	10	TFA	84	47:53	85, 83
9	96–120	2.5	10	TFA	78	48:52	73, 71
10	120–150	2.5	10	TFA	77	49:51	77, 73
11	150–170	2.5	10	TFA	60	49:51	75, 74

[a] Isolated yield after chromatographic purification. [b] Evaluated by ^{1}H NMR spectroscopy on the crude reaction mixture. [c] Evaluated by HPLC on a chiral stationary phase after reduction to the corresponding alcohol (see the Supporting Information).

Table 5. Diels–Alder reaction promoted by catalyst type **A10-1** under continuous-flow conditions.

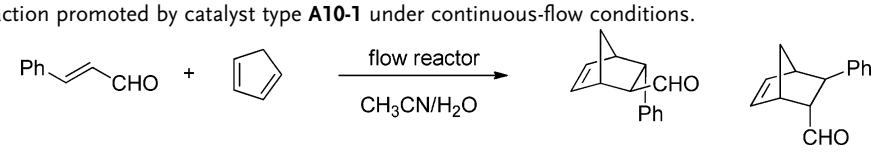

Entry	*t* [h]	Flow rate [μL/min]	Residence time [h]	HX	Yield [%][a]	*endo*/*exo*[b]	*ee* [%] (*endo*,*exo*)[c]
1	10–24	2.5	10	HBF_4	54	n.d	n. d.
2	24–48	2.5	10	HBF_4	76	52 : 48	71, 68
3	48–72	2.5	10	HBF_4	76	51 : 49	69, 66
4	72–96	2.5	10	HBF_4	60	51 : 49	68, 58
5	10–24	2.5	10	TFA	60	62 : 37	60, 80
6	24–48	2.5	10	TFA	50	53 : 47	67, 70
7	48–72	2.5	10	TFA	32	52 : 48	68, 70
8	72–96	2.5	10	TFA	25	53 : 47	63, 63

[a] Isolated yield after chromatographic purification. [b] Evaluated by ^{1}H NMR spectroscopy on the crude reaction mixture. [c] Evaluated by HPLC on a chiral stationary phase after reduction to the corresponding alcohol (see the Supporting Information).

higher than 80 %, working for more than 150 h with high stereochemical efficiency; it must be said that, after 96 h, to maintain the production over a threshold of 90 % yield it was necessary to further slow down the flow rate; thus increasing the retention time (Table 4, entry 6).

When the trifluoroacetate salt of supported imidazolidinone **A8-1** was employed, it was observed that the column reached a high efficiency in a shorter time than the tetrafluoroborate salt. After 10 h only, the products were obtained in 94 % yield and 85 % *ee* (Table 4, entry 5); however, it was also observed that the catalytic efficiency started to decrease after 96 h only (Table 4, entry 7).

The influence of the morphological characteristics of the material on the catalytic activity was then studied. Therefore, silica nanoparticles of different sizes were employed; in Table 5 selected results of the cycloaddition performed in flow in a catalytic reactor filled with functionalized 10 μm silica nanoparticles are reported (catalyst **A10-1**). By comparing the activities of the trifluoroacetate and the tetrafluoroborate salts, the same behavior as the previous columns with 8 μm particles was observed: longer times were required by the HBF_4 salt to reach a constant level of catalytic efficiency; with TFA-treated supported imidazolidinones higher *ee* were produced (Table 5, entries 5–8 versus entries 1–4). However, the catalytic columns filled with catalyst **A8-1** performed generally better than those loaded with **A10-1**-type silica-supported catalysts, both in terms of chemical and stereochemical efficiency.

Based on these data, two other types of silica-supported catalysts were prepared by using 8 μm silica particles, but with lower chiral catalyst loadings than **A8-1**. The performances of the two new HPLC columns (filled with materials **A8-2** and **A8-3**) in the model cycloaddition of cinnamic aldehyde to cyclopentadiene under continuous-flow conditions were evaluated, and compared to the data obtained with the reactor containing catalyst **A8-1**.

A few selected results are briefly summarized in Table 6. It is clear that lower loadings dramatically reduced the activity of the catalytic columns. The **A8-2**-supported catalyst (loading 0.3 mmol/g vs. loading of 0.4 mmol/g of catalyst **A8-1**) employed in flow promoted the Diels–Alder reaction in lower yields and enantioselectivities than **A8-1**. Silica-supported catalysts **A8-3** showed almost no appreciable catalytic activity (Table 6, entries 4–6 and entries 7–9).

Finally, the nature of the material and the immobilization strategies were also taken in consideration. Type **B** catalysts were prepared by exploiting the click chemistry approach; in the case of material **B1** commercially available silica nanoparticles were employed, whereas for catalysts **B2** ad hoc synthesized mesoporous silica nanoparticles were used (Scheme 3).

Surprisingly, when the cycloaddition reaction was performed in continuo by pumping the reagents in a column loaded with material **B1**, neither unreacted starting materials nor products were observed, even after prolonged fluxing of the reactor (six volumes of column were flushed into the column, see the comments of the SEM images). However, when the column was discharged and the recovered silica was suspended in CH_2Cl_2 and stirred for 1 h, evaporation of the filtered organic phase afforded the expected cycloadducts in 95 % yield and 90 % *ee* for both isomers. Extensive particle aggregation evidenced by SEM images may partially account for the unusual behavior of the column that seemed to entrap the organic molecules.

On the other hand, it was possible to perform organocatalyzed reactions under continuous-flow conditions with catalyst type **B2**. The results are reported in Table 7.

The catalytic column loaded with mesoporous functionalized silica **B2** was able to continuously produce the cy-

Table 6. Comparison of the catalytic behavior of materials **A8-1**, **A8-2**, and **A8-3** in Diels–Alder reactions under continuous-flow conditions.

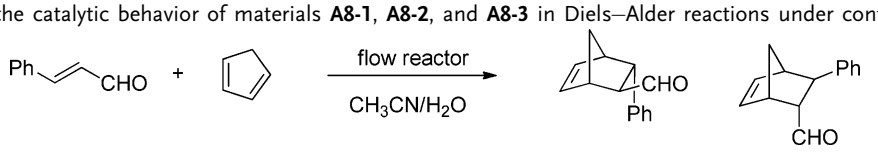

Entry	*t* [h]	Flow rate [μL/min]	Residence time [h]	Catalyst	Yield [%][a]	*endo*/*exo*[b]	*ee* [%] (*endo*,*exo*)[c]
1	10–30	2.5	10	**A8-1**	55	46 : 54	40, 60
2	30–50	1.5	16.5	**A8-1**	91	47 : 53	71, 73
3	50–96	1.5	16.5	**A8-1**	92	42 : 58	85, 81
4	10–30	2.5	10	**A8-2**	31	49 : 51	n.d.
5	30–50	1.5	16.5	**A8-2**	41	48 : 52	46, 56
6	50–72	1.5	16.5	**A8-2**	21	51 : 49	45, 55
7	10–30	2.5	10	**A8-3**	11	50 : 50	n.d.
8	30–50	1.5	16.5	**A8-3**	15	53 : 47	43, 47
9	50–96	1.5	16.5	**A8-3**	12	51 : 49	n.d.

[a] Isolated yield after chromatographic purification. [b] Evaluated by ^{1}H NMR spectroscopy on the crude reaction mixture. [c] Evaluated by HPLC on a chiral stationary phase after reduction to the corresponding alcohol (see the Supporting Information).

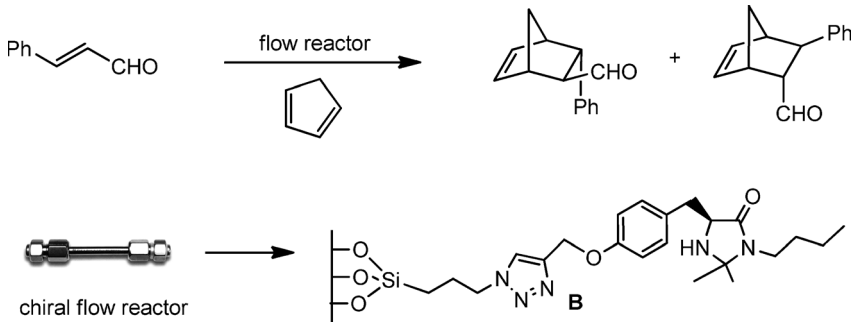

Scheme 3. Use of supported catalysts **B** under continuous-flow conditions.

Table 7. Diels–Alder reaction promoted by catalyst **B2** under continuous-flow conditions.

Entry	*t* [h]	Flow rate [μL/min]	Residence time [h]	HX	Yield [%][a]	*endo*/*exo*[b]	*ee* [%] (*endo*,*exo*)[c]
1	10–30	2.5	10	HBF_4	60	50 : 50	74, 91
2	30–50	2.5	10	HBF_4	50	47 : 53	80, 94
3	50–72	2.5	10	HBF_4	35	49 : 51	82, 97

[a] Isolated yield after chromatographic purification. [b] Evaluated by ^{1}H NMR spectroscopy on the crude reaction mixture. [c] Evaluated by HPLC on a chiral stationary phase after reduction to the corresponding alcohol (see the Supporting Information).

cloadducts with high enantioselectivities (up to 97 %), but in lower yield than catalyst **A8-1**. Also, it is worth mentioning that material **B2** seems to rapidly lose catalytic activity; after 50 h, although the level of enantioselection remains very high, the chemical yield shows a clear decrease (Table 7, entries 2 and 3).

All data for the catalytic behavior of the different columns are summarized in Figure 6. The curves are intended to fit the data reported in Tables 4–7 and to show the trends of conversions and enantioselectivities during the reactions performed under continuous-flow conditions. Figure 6a reports the conversions at different reaction times: it is clearly evidenced how catalyst **A8-1** maintained a higher chemical efficiency than the other materials for longer operation times. Figure 6b illustrates the enantioselectivities guaranteed by the different supported catalysts, highlighting the excellent performances of materials **A8-1** and **B2**, but with the second one penalized by a quick chemical deactivation (see Figure 6a).

Finally, it is worth mentioning that the regeneration of the catalytic column is possible. A used HPLC column filled with tetrafluoroborate salt (after 180 working hours) was first washed with aqueous acetonitrile, and then fluxed with 0.33 mL of an aqueous solution of HBF_4 in acetonitrile. The regenerated catalytic column was employed again in the cycloaddition of cyclopentadiene with cinnamic aldehyde (Table 8). Longer times were necessary to reach satisfactory conditions at steady-state regime

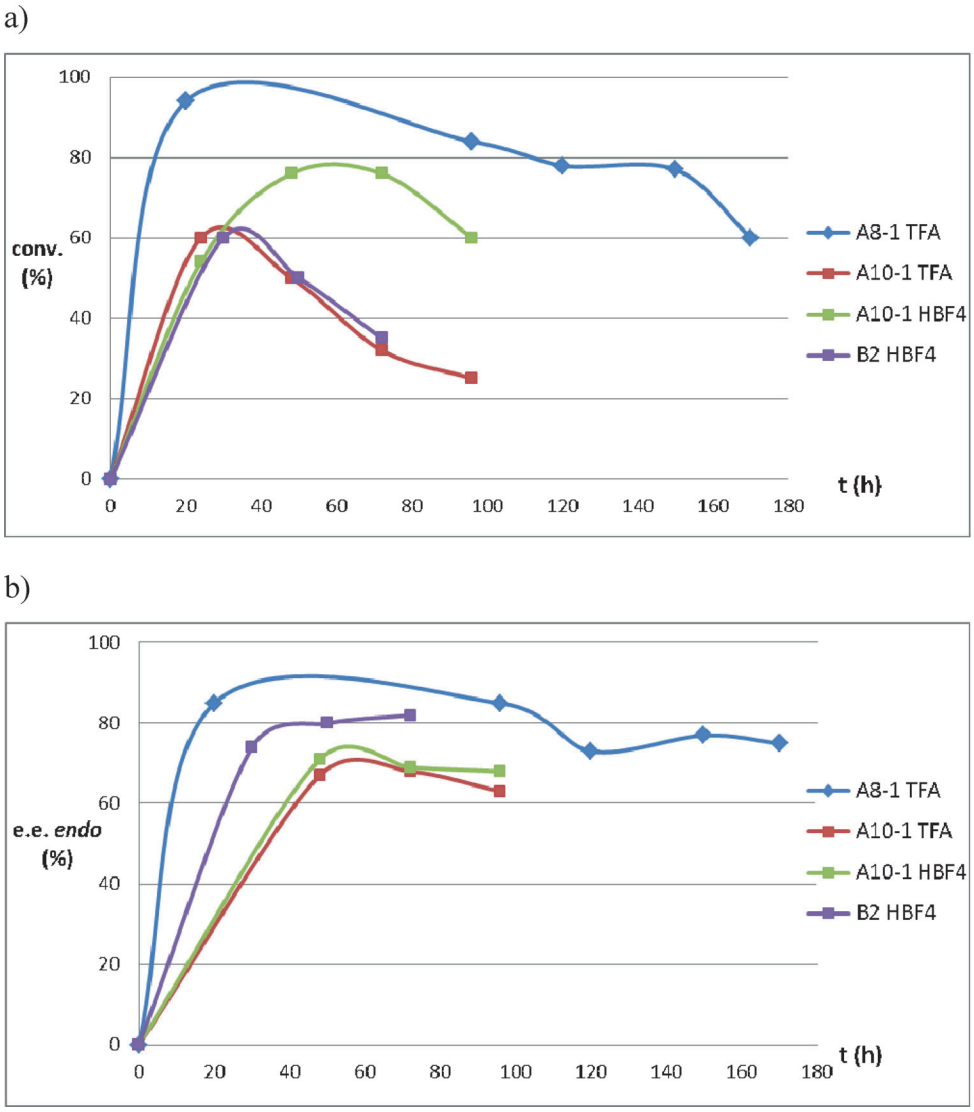

Figure 6. Comparison of yields and *ee* obtained with different catalytic columns. Steady flow rates (2.5 μL/min) and residence times (10 h) were used for all reported catalysts.

(Table 8, entries 1 and 2). However, after 30 h the products were collected in yields comparable to those obtained with a freshly prepared reactor.[29] Notably, if one considers the performance of the catalytic column before and after regeneration, the simple homemade catalytic reactor was demonstrated to work for more than 300 h under continuous-flow conditions.

Figure 7 shows how, after the regeneration procedure, the chemical activity of the column may be restored, although it must be said that it was necessary to set up a longer residence time for the regenerated column to guarantee yields of $>85\,\%$.

Further studies are underway to investigate the origin of catalyst deactivation to optimize flow reaction conditions and to improve the applicability of the chiral columns.

Finally, it is interesting to compare some results obtained in the organocatalyzed cycloaddition performed with supported catalysts in batch or under continuous-flow conditions; the data are collected in Table 9, in which TON and productivity of the different materials are reported.

Considering the results obtained with the TFA salt of **A8-1** in batch after 48 h, the TON (calculated as mmol of product per mmol of catalyst) is 2.3, while in flow almost a threefold increase was obtained. For longer times, the process in flow offers even better performances; a clear advantage over the batch process, reaching a TON of 24.4 after 170 h. Outstandingly, for the trifluoroacetate salt of supported imidazolidinone **A8-1** a remarkable value of productivity, 143, was calculated (as mmol of product per mmol of catalyst per hour).

Table 8. Catalytic behavior of a regenerated chiral reactor under continuous-flow conditions.

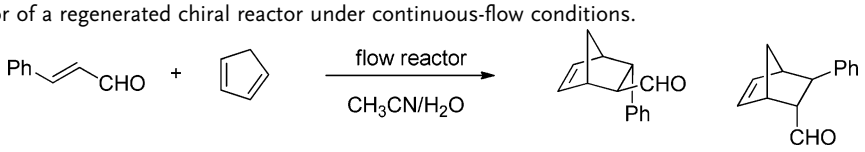

Entry	*t* [h]	Flow rate [µL/min]	Residence time [h]	HX	Yield [%][a]	*endo*/*exo*[b]	*ee* [%] (*endo*,*exo*)[c]
1	0–20	1.5	16.5	HBF_4	40	48 : 52	60, 57
2	20–30	1.5	16.5	HBF_4	55	49 : 51	71, 75
3	30–50	1.5	16.5	HBF_4	87	48 : 52	80, 73
4	50–168	1.5	16.5	HBF_4	85	47 : 53	75, 71
5	168–192	2.5	10	TFA	78	48 : 52	70, 66

[a] Isolated yield after chromatographic purification. [b] Evaluated by ^{1}H NMR spectroscopy on the crude reaction mixture. [c] Evaluated by HPLC on chiral stationary phase after reduction to the corresponding alcohol (see the Supporting Information).

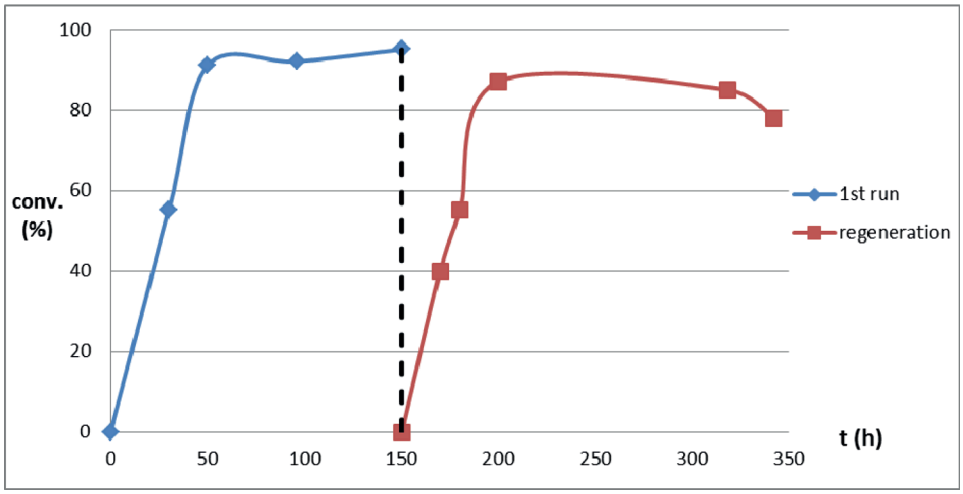

Figure 7. Representation of conversion versus time of a catalytic reactor before and after regeneration.

Table 9. A comparison of batch and continuous-flow conditions.

Entry	Catalyst	*t* [h]	Productivity[a]	TON[b] Batch 48 h	TON[b] Flow 48 h	TON[b] Flow total
1	**A8-1** (TFA)	170	143	2.3	6.3	24.4 (170 h)
2	**A8-1** (HBF_4)	150	44	2.5	2.1	6.5 (150 h) 12.3 (342 h)
3	**A10-1** (TFA)	120	33	2.2	1.9	3.2 (120 h)
4	**A10-1** (HBF_4)	96	57	2.6	2.4	5.4 (96 h)
5	**B2** (HBF_4)	72	41	2.5	1.1	2.9 (72 h)

[a] Productivity is measured in mmol(product) h^{-1} mmol(catalyst)$^{-1}\times10^3$. [b] Turnover number (TON) is measured in mmol(product) mmol(catalyst)$^{-1}$.

With the tetrafluoroborate salt, which behaved better in batch, for long operation times, the flow process favorably compares with the reaction performed in a flask; regeneration of the column allowed the TON to be further increased up to 12.3.

3 Conclusion

Silica nanoparticles of different morphological properties were functionalized with enantiomerically pure imidazolidinones, through different immobilization techniques, including grafting and click cycloaddition-based strategies. Stainless-steel columns were then loaded with silica bearing the chiral organocatalysts to realize chiral "homemade" reactors and their catalytic behavior was studied

by performing a model Diels–Alder reaction between cyclopentadiene and cinnamic aldehyde. By operating under the best experimental conditions, it was demonstrated that a simple HPLC column, filled with commercially available silica-supported MacMillan catalyst, may work as a catalytic reactor for 150 h, affording the product in high yields and enantioselectivities. A regeneration procedure may restore the catalytic efficiency of the column, allowing the activity of the reactor to be further extended to more than 300 operating hours. The flow process performed clearly better than the batch process, and reached a TON of 24 (against 2.3 for the batch) and 143 of productivity. Additionally, it should be considered that the continuous-flow methodology does not require any workup, separation, and recovery operations; this allows for the easy isolation of the reaction products in a time-saving procedure.

Although TON and reaction rates need to be improved, it was already demonstrated that the process in continuo may positively compete with the reaction in batch, affording, in the same time, larger amounts of product, in a user-friendly experimental procedure, which leads to cleaner crude reaction mixtures.

Experimental Section

Materials

Trimethoxysilane (Aldrich reagent grade 99%), TEOS (Aldrich reagent grade 98%), CTAB (Sigma reagent grade 98%) and chloroplatinic acid ($H_2PtCl_6 \cdot 6H_2O$; Aldrich ACS reagent) were purchased from Sigma-Aldrich and used without further purification.

All reactions were carried out in oven-dried glassware with magnetic stirring under a nitrogen atmosphere, unless otherwise stated. Dry solvents were purchased and stored under nitrogen over molecular sieves (bottles with crown caps). Reactions were monitored by analytical TLC using silica gel 60 F_{254} pre-coated glass plates (0.25 mm thickness) and visualized using UV light or phosphomolybdic acid.

NMR Spectroscopy

The ^1H and ^{13}C NMR spectra were recorded on a Bruker Avance 500 spectrometer operating at 500.0 and 125.62 MHz, respectively. The spectra are performed in $CDCl_3$ and the chemical shifts externally referenced to tetramethylsilane (TMS).

Solid-State NMR Spectroscopy

The ^{13}C and ^{29}Si solid-state NMR spectra were recorded at 125.62 and 99.36 MHz, respectively, on a Bruker Avance 500 spectrometer, equipped with a 4 mm MAS broad-band probe (spinning rate, n_R, up to 13 kHz). The MAS spectra were performed on solid samples (typically 0.12 g); each sample was packed into a 4 mm MAS rotor (50 ml sample volume) spinning at 13 kHz and at a temperature of 300 K. DP and variable-amplitude CP methods (contact time, t_c, 1 ms) were used for recording the ^{29}Si spectra with 400 scans and a delay of 300.0 s and 20000 scans and a delay of 3.0 s, respectively. The ^{13}C experiments were performed with the CP method using a contact time, t_c, of 1.5 ms, 70000 scans, and 3.0 s of delay. All chemical shifts were externally referenced to TMS.

The ^{29}Si resonances were assigned following previous reports in the literature,[26] while those of ^{13}C were referred to the chemical shifts found in the solution spectra of the corresponding unbound compounds.

Scanning Electron Microscopy

SEM micrographs were obtained by using a Zeiss SIGMA FE-SEM instrument operating at 0.2–30 kV. The powder samples were coated with gold before analysis.

Synthesis of 5-MSN

A solution of CTAB (365 mg, 1 mmol) in water (88 mL) and 2M NaOH (1.3 mL) was mechanically stirred at 550 rpm at 80 °C for 30 min. The stirring speed was decreased to 200 rpm and TEOS (1.82 mL, 8.16 mmol) and siloxane **4** (0.26 g, 1.05 mmol) were rapidly added. After 2 min stirring at 200 rpm a precipitate was formed. Stirring at 500–600 rpm was continued for 2.0 h at 80 °C and the mixture was filtered while still hot. The solid was washed with water (150 mL) and MeOH (150 mL), and dried under high vacuum for 3 h to afford a white material (794 mg). This was then treated with a solution of concentrated HCl (0.6 mL) in MeOH (80 mL) under mechanical stirring for 2.5 h at 60 °C to remove the surfactant. The cooled mixture was filtered and the solid was washed again with water and MeOH (100 mL each). The white solid was dried under high vacuum for 3 h at 90 °C and subjected to alkaline wash with saturated a solution of Na_2CO_3 in methanol (100 mL/g). After 3 h of stirring at 550 rpm at room temperature, the mixture was filtered and the solid was washed with water and methanol and dried under high vacuum at 80 °C for 3 h. The material was finally suspended in distilled water (100 mL/g) and mechanically stirred at 550 rpm at room temperature for 2 h, filtered on a porous septum, washed with methanol, and dried under high vacuum at 60 °C to give a constant weight.

Synthesis of 2

Imidazolidinone **2** was prepared according to a published procedure.[16]

Preparation of Imidazolidinone 3

To a stirred portion of butylamine (10 mL, 101.2 mmol) kept under nitrogen, (*S*)-tyrosine methyl ester (6 g, 30.8 mmol) was added and the mixture was stirred for 24 h at room temperature. After addition of CH_2Cl_2, the

reaction was evaporated under vacuum to give a pale yellow solid (7.2 g) that was used for the next reaction without any further purification step. The compound was dissolved in CH_3OH (60 mL) and acetone (60 mL), and PTSA (60 mg) was added. The mixture was heated at reflux for 24 h and concentrated under vacuum to afford the crude imidazolidinone (8.4 g), which was used for the next reaction without any further purification step. M.p. 99–101 °C; $[\alpha]_D^{23} = -78.2$ ($c = 0.72$ in CH_2Cl_2); ^{1}H NMR ($CDCl_3/D_2O$): $\delta = 7.04$ (B part of AB system, ^3J (H,H) = 8.5 Hz, 2H; aromatic protons), 6.74 (A part of AB system, ^3J (H,H) = 8.5 Hz, 2H; aromatic protons), 3.73 (t, ^3J (H,H) = 5.8 Hz, 1H; CHN), 3.29 (ddd, ^2J (H,H) = 12.0 Hz, ^3J (H,H) = 6.7 and 3.2 Hz, 1H; one H of NCH_2), 3.04 (ddd, ^2J (H,H) = 12.0 Hz, ^3J (H,H) = 5.8 and 5.4 Hz, 2H; $ArCH_2$), 2.89 (ddd, ^2J (H,H) = 12.0 Hz, ^3J (H,H) = 6.2 and 3.1 Hz, 1H; one H of NCH_2), 1.43–1.49 (m, 2H; NCH_2CH_2), 1.21–1.31 (m, 2H; CH_3CH_2), 1.27 (s, 3H; CMe), 1.17 (s, 3H; CMe), 0.90 ppm (t, ^3J (H,H) = 7.3 Hz, 3H; CH_2CH_3); ^{13}C NMR: $\delta = 174.2$, 155.8, 130.7, 127.2, 115.7, 76.4, 58.9, 40.4, 35.5, 31.3, 27.8, 26.3, 20.3, 13.7 ppm; IR: 3270, 1675, 1620 cm^{-1}; elemental analysis calcd (%) for $C_{16}H_{24}N_2O_2$ (276.4): C 69.53, H 8.75, N 10.14; found: C 69.71, H 8.64, N 10.23.

To a solution of the crude imidazolidinone (5 g, 18 mmol) in dry acetonitrile (40 mL), potassium carbonate (20 g, 145 mmol) was added and the mixture was cooled to 0 °C with an external ice water bath; propargyl bromide solution (80 wt% in toluene, 8 mL, 72 mmol) was added dropwise over 15 min and the resulting mixture was allowed to warm to room temperature and stirred under an inert atmosphere for 24 h. The reaction mixture was then filtered through a Celite plug and the solvent was removed under vacuum; the crude product was purified by flash column chromatography (eluent: CH_2Cl_2/MeOH = 98/2) to afford compound **3** as a brownish oil (15.9 mmol, 88%). $R_f = 0.47$ (CH_2Cl_2/MeOH = 98/2); ^{1}H NMR (300 MHz, $CDCl_3$): $\delta = 7.12$ (d, 2H; Ar-H), 6.85 (d, 2H; Ar–H), 4.59 (d, 2H; –O–CH_2), 3.65 (t, 1H; –NH–CH–), 3.23–3.20 (m, 1H; –N–CH_2–), 2.97 (dd, 2H; Ar–CH_2–), 2.96–2.84 (m, 1H; –N–CH_2–), 2.46 (t, 1H; –C≡CH), 1.41 (m, 2H; –N–CH_2–CH_2–), 1.29–1.24 (m, 2H; CH_2–CH_3), 1.20 (s, 3H; –C–CH_3), 1.09 (s, 3H; –C–CH_3), 0.86 ppm (t, 3H; –CH_2–CH_3); ^{13}C NMR (75 MHz, $CDCl_3$): $\delta = 174.1$ (1C, –C=O), 156.8 (1C, Ar–C–O–), 131.0 (2C, Ar–CH), 130.1 (1C, Ar–C–), 115.2 (2C, Ar–CH), 78.8 (1C, –C≡CH), 76.3 (1C, –N–C–NH-), 75.7 (1C, –C≡CH), 59.1 (1C, –NH–CH–C=O), 56.1 (1C, –O–CH_2–), 40.5 (1C, –N–CH_2–), 36.2 (1C, Ar–CH_2–), 31.7 (1C, –N–CH_2–CH_2–), 28.3 (1C, –C–CH_3), 26.8 (1C, –C–CH_3), 20.6 (1C, –CH_2–CH_3), 14.0 ppm (1C, –CH_2–CH_3).

General Procedure for the Grafting Reaction (Catalysts A8-1, A8-2, A8-3, and A10)

Commercial silica particles (1 g) and the properly modified organotrimethoxysilane (2 mmol) were suspended in toluene (10 mL) and allowed to stir under an inert atmosphere at reflux for 48 h. The supported catalyst was isolated by centrifugation, washed with CH_2Cl_2 (2 × 10 mL), and dried under vacuum.

General Procedure for the Click Reaction (Catalysts B1 and B2)

The azide-derived siliceous material (1 g) and imidazolidinone derivative 3 (1.56 mmol) were suspended in tetrahydrofuran (10 mL) and allowed to stir in the presence of DIPEA (15 mmol) and copper(I) iodide (0.01 mmol) at 35 °C for 40 h. The supported catalyst was isolated by centrifugation, washed with CH_2Cl_2 (2 × 10 mL), with ammonia solution (15 mL), and dried under high vacuum.

Catalysis: General Procedure

The continuous-flow packed-bed reactor was prepared filling a stainless-steel HPLC column (length 12.5 cm, i.d. 0.4 cm) with 1 g of silica-supported imidazolidinone catalyst (A or B). It was flow-treated with TFA solution (0.2M in 10 mL of a 95/5 CH_3CN/H_2O mixture) or with a 48% solution in water of HBF_4 (0.2M, in 10 mL of a 95/5 CH_3CN/H_2O mixture). The Diels–Alder cycloaddition reaction was then carried out at 25 °C by pumping a solution of the reagents (*trans*-cinnamaldehyde (2.5 mmol) and cyclopentadiene (17 mmol) in a 95/5 CH_3CN/H_2O mixture (10 mL)) through the reactor by a syringe pump. After 48 h of operation the flow was stopped, the syringe was recharged with freshly distilled cyclopentadiene and cinnamic aldehyde (to limit reagents degradation), and the flow was started again.

The *endo*/*exo* ratio was established on the crude product by using the CHO signals at $\delta = 9.60$ (*endo*) and 9.93 (*exo*) ppm. This product is known[16] and was purified by flash column chromatography on silica gel with 8:2 hexane/ethyl acetate as the eluant, affording a mixture of *endo* and *exo* Diels–Alder adducts. For *ee* determination, the aldehyde was converted into the corresponding alcohol by reduction with an excess of $NaBH_4$ in CH_3OH, at 24 °C, for 1 h.

Supporting Information Available. The contents of Supporting Information include the following: synthetic details for the preparation of functionalized materials, NMR spectra of functionalized silica particles, analytical data of the non-supported catalysts, NMR and HPLC spectra of the cycloadducts.

Acknowledgments

This work was supported by MIUR-PRIN (Nuovi metodi catalitici stereoselettivi e sintesi stereoselettiva di molecole funzionali), the Cariplo Foundation (Milano) within the project 2011-0293 “Novel chiral recyclable catalysts for one-pot, multi-step synthesis of structurally complex molecules”, and FIRB project RBFR10BF5V “Multifunctional hybrid materials for the development of sustainable catalytic processes”. M. B. thanks COST action CM9505

"ORCA" Organocatalysis. We thank Angelo Magri (T. F. B.) for technical support.

References

[1] a) G. Jas, A. Kirschning, *Chem. Eur. J.* **2003**, *9*, 5708–5723; b) B. P. Mason, K. E. Price, J. L. Steinbacher, A. R. Bogdan, D. T. McQuade, *Chem. Rev.* **2007**, *107*, 2300–2318; c) C. Wiles, P. Watts, *Eur. J. Org. Chem.* **2008**, 1655–1671.

[2] A. Solinas, M. Taddei, *Synthesis*, **2007**, 2409–2433.

[3] A. Kirschning, W. Solodenko, K. Mennecke, *Chem. Eur. J.* **2006**, *12*, 5972–5990.

[4] a) S. V. Ley, I. R. Baxendale, *Chimia*, **2008**, *62*, 162–168; d) B. Ahmed-Omer, J. C. Brandt, T. Wirth, *Org. Biomol. Chem.* **2007**, *5*, 733–740.

[5] For recent publications, see selected references: a) *Microreactors in Organic Synthesis and Catalysis* (Ed.: T. Wirth), Wiley-VCH, Weinheim, **2008**; b) V. Hessel, *Chem. Eng. Technol.* **2009**, *32*, 1655–1681; c) J. Wegner, S. Ceylan, A. Kirschning, *Chem. Commun.* **2011**, 4583–4592; d) S. Ceylan, L. Coutable, J. Wegner, A. Kirschning, *Chem. Eur. J.* **2011**, *17*, 1884–1893; e) R. L. Hartman, J. P. McMullen, K. F. Jensen, *Angew. Chem. Int. Ed.* **2011**, *50*, 7502–7519; f) C. Wiles, P. Watts, *Green Chem.* **2012**, *14*, 38–54.

[6] For the application of flow chemistry for multistep organic synthesis, see: a) J. Wegner, S. Ceylan, A. Kirschning, *Adv. Synth. Catal.* **2012**, *354*, 17–57; b) M. Baumann, I. R. Baxendale, S. V. Ley, *Mol. Diversity* **2011**, *3*, 613–630; for some recent, representative contributions, see: c) M. Chen, S. Buchwald, *Angew. Chem. Int. Ed.* **2013**, *52*, 4247–4250; d) I. R. Baxendale, S. V. Ley, A. C. Mansfield, C. D. Smith, *Angew. Chem. Int. Ed.* **2009**, *48*, 4017–4021.

[7] For some recent selected books and reviews, see: a) K. Geyer, T. Gustafson, P. H. Seeberger, *Synlett* **2009**, 2382–2391; b) C. Wiles, P. Watts, *Chem. Commun.* **2011**, 6512–6521; c) R. M. Myers, K. A. Roper, I. R. Baxendale, S. V. Ley in *Modern Tools for the Synthesis of Complex Bioactive Molecules* (Eds.: J. Cossy, S. Arseniyadis), Wiley, New York, **2012**, Chapter 11, pp. 359–394; d) S. G. Newman, K. F. Jensen, *Green Chem.* **2013**, *15*, 1456–1472.

[8] a) *Recoverable and Recyclable Catalysts* (Ed.: M. Benaglia), Wiley, Chichester, **2009**; b) N. Haraguchi, S. Itsuno, *Polymeric Chiral Catalyst Design and Chiral Polymer Synthesis*, Wiley, Hoboken, **2011**; c) *Handbook of Asymmetric Heterogeneous Catalysts* (Eds.: K. J. Ding, F. J. K. Uozomi), Wiley-VCH, Weinheim, **2008**; for reviews on supported organic catalysts, see: d) F. Cozzi *Adv. Synth. Catal.* **2006**, *348*, 1367; e) M. Benaglia, *New J. Chem.* **2006**, *30*, 1525.

[9] a) C. G. Frost, L. Mutton, *Green Chem.* **2010**, *12*, 1687–1703; b) T. Tsubogo, T. Ishiwata, S. Kobayashi, *Angew. Chem. Int. Ed.* **2013**, *52*, 6590–6604.

[10] A. Puglisi, M. Benaglia, V. Chiroli, *Green Chem.* **2013**, *15*, 1790–1813.

[11] A. M. Hafez, A. E. Taggi, T. Dudding, T. Lectka, *J. Am. Chem. Soc.* **2001**, *123*, 10853–10859.

[12] a) E. Alza, C. Rodríguez-Escrich, S. Sayalero, A. Bastero, M. A. Pericàs, *Chem. Eur. J.* **2009**, *15*, 10167–10172; b) C. Ayats, A. H. Henseler, M. A. Pericàs, *ChemSusChem* **2012**, *5*, 320–325.

[13] a) E. Alza, S. Sayalero, X. C. Cambeiro, R. Martin-Rapun, P. O. Miranda, M. A. Pericàs, *Synlett* **2011**, 464–468; b) X. Fan, S. Sayalero, M. Pericàs, *Adv. Synth. Catal.* **2012**, *354*, 2971–2976; c) O. Bortolini, L. Caciolli, A. Cavazzini, V. Costa, R. Greco, A. Massi, L. Pasti, *Green Chem.* **2012**, *14*, 992–1000; d) O. Bortolini, A. Cavazzini, P. Giovannini, R. Greco, N. Marchetti, A. Massi, L. Pasti, *Chem. Eur. J.* **2013**, *19*, 7802–7808, and references cited.

[14] S. B. Otvos, I. M. Mandity, F. Fulop, *ChemSusChem* **2012**, *5*, 266–269, and references cited.

[15] Y. Arakawa, H. Wennemers, *ChemSusChem* **2013**, *6*, 242–245.

[16] V. Chiroli, M. Benaglia, F. Cozzi, A. Puglisi, R. Annunziata, G. Celentano, *Org. Lett.* **2013**, *15*, 3590–3593.

[17] G. Lelais, D. W. C. MacMillan, *Aldrichimica Acta* **2006**, *39*, 79–87.

[18] a) M. Benaglia, G. Celentano, M. Cinquini, A. Puglisi, F. Cozzi, *Adv. Synth. Catal.* **2002**, *344*, 149–152; b) A. Puglisi, M. Benaglia, M. Cinquini, F. Cozzi, G. Celentano, *Eur. J. Org. Chem.* **2004**, 567; c) S. Guizzetti, M. Benaglia, J. S. Siegel, *Chem. Commun.* **2012**, *48*, 3188–3190.

[19] S. A. Selkälä, J. Tois, P. M. Pihko, A. M. P. Koskinen, *Adv. Synth. Catal.* **2002**, *344*, 941.

[20] Y. Zhang, L. Zhao, S. S. Lee, J. Y. Ying, *Adv. Synth. Catal.* **2006**, *348*, 2027.

[21] H. Hagiwara, T. Kuroda, T. Hoshi, T. Suzuki, *Adv. Synth. Catal.* **2010**, *352*, 909.

[22] J. Y. Shi, C. A. Wang, Z. J. Li, Q. Wang, Y. Zhang, W. Wang, *Chem. Eur. J.* **2011**, *17*, 6206.

[23] a) P. Riente, J. Yadav, M. A. Pericàs, *Org. Lett.* **2012**, *14*, 3668; b) S. Mondini, A. Puglisi, M. Benaglia, D. Ramella, C. Drago, A. M. Ferretti, A. Ponti, *J. Nanopart. Res.* **2013**, *15*, 2025.

[24] a) A. Puglisi, R. Annunziata, M. Benaglia, F. Cozzi, A. Gervasini, V. Bertacche, M. C. Sala, *Adv. Synth. Catal.* **2009**, *351*, 219; b) A. Puglisi, M. Benaglia, R. Annunziata, V. Chiroli, R. Porta, A. Gervasini, *J. Org. Chem.* **2013**, *78*, 11326.

[25] It is known that residual copper can lead to an erosion of the enantiomeric excess in stereoselective catalyzed reactions, see for example: a) A. Gissibl, M. G. Finn, O. Reiser, *Org. Lett.* **2005**, *7*, 2325; the same authors also showed that unbound copper does not interfere with the stereochemical activity of the catalyst if the ligand is supported on globular supports and magnetic nanoparticles: b) A. Gissibl, C. Padie, M. Hager, F. Jaroschik, R. Rasappan, E. Cuevas-Yan ez, C.-O. Turrin, A.-M. Caminade, J.-P. Majoral, O. Reiser, *Org. Lett.* **2007**, *9*, 2895; c) A. Schatz, M. Hager, O. Reiser, *Adv. Funct. Mater.* **2009**, *19*, 2109.

[26] a) S. Huh, J. W. Wiench, Y. Wi-Chul, M. Pruski, V. S.-Y. Lin, *Chem. Mater.* **2003**, *15*, 4247; b) S. Huh, H. T. Chen, J. W. Wiench, M. Pruski, V. S.-Y. Lin, *Angew. Chem. Int. Ed.* **2005**, *44*, 1826.

[27] For detailed reaction procedures, product analysis, and *ee* determination, see the Experimental Section and the Supporting Information.

[28] K. A. Ahrendt, C. J. Borths, D. W. C. MacMillan, *J. Am. Chem. Soc.* **2000**, *122*, 4243.

[29] For experimental details, see ref. [16].

Received: September 12, 2013
Accepted: January 13, 2014
Published online: March 20, 2014